Reaction pathway, energy barrier, and rotational state distribution for $Li(2\,^2P_J)+H_2 \rightarrow LiH(X\,^1\Sigma^+)+H$

Jye-Jong Chen, Yu-Ming Hung,[a] Dean-Kuo Liu, Hok-Sum Fung, and King-Chuen Lin[b]
Department of Chemistry, National Taiwan University, Taipei, Taiwan, Republic of China and Institute of Atomic and Molecular Sciences, Academia Sinica, P.O. Box 23-166, Taipei 106, Taiwan, Republic of China

(Received 28 November 2000; accepted 16 March 2001)

By using a pump-probe technique, we have observed the nascent rotational population distribution of $LiH(v=0)$ in the $Li(2\,^2P_J)$ with a H_2 reaction, which is endothermic by 1680 cm^{-1}. The $LiH(v=0)$ distribution yields a single rotational temperature at ~770 K, but the population in the $v=1$ level is not detectable. According to the potential energy surface (PES) calculations, the insertion mechanism in (near) C_{2v} collision geometry is favored. The $Li(2\,^2P_J)-H_2$ collision is initially along the $2A'$ surface in the entrance channel and then diabatically couples to the ground $1A'$ surface, from which the products are formed. From the temperature dependence measurement, the activation energy is evaluated to be $1280\pm46\,cm^{-1}$, indicating that the energy required for the occurrence of the reaction is approximately the endothermicity. As Li is excited to higher states ($3\,^2S$ or $3\,^2P$), we cannot detect any LiH product. From a theoretical point of view, the $4A'$ surface, correlating with the Li $3\,^2S$ state, may feasibly couple to a repulsive $3A'$ surface, from which the collision complex will rapidly break apart into $Li(2\,^2P_J)$ and H_2. The probability for further surface hopping to the $2A'$ or $1A'$ surfaces is negligible, since the $3A'$ and $2A'$ surfaces are too far separated to allow for an efficient coupling. The $Li(3\,^2P)$ state is expected to behave similarly. The observation also provides indirect evidence that the harpoon mechanism is not applicable to this system. © *2001 American Institute of Physics.* [DOI: 10.1063/1.1370070]

I. INTRODUCTION

Reaction dynamics of electronically excited alkali atoms with the hydrogen molecule has become an attractive topic for study for decades.[1–10] The advent of the tunable laser makes it feasible to deposit excitation energies in various atomic states, which are large enough to overcome the energy requirements of endothermic reactions. Among the issues of reaction dynamical complexity having been studied, the reaction pathway is an issue of common concern. Thus far, the reaction pathways for K,[7,8,11–15] Rb,[16,17] and Cs[1,3,9,18–23] are found to be similar, proceeding via a harpoon mechanism in a (near) collinear collision, whereas Na[4,5,10] prefers an insertion mechanism.

In a series of reaction studies with the hydrogen molecule for excited states of Cs by Vetter and Bersohn,[1,3,9,18–23] K by Lin and Kleiber,[7,8,11–15] and Rb by Luh[16,17] and their co-workers, the following results were found. First, the reactions followed a colinear collisional geometry, producing alkali hydrides predominantly via an ion-pair intermediate; however, for the case of Cs, an electron jumping distance was shorter than the harpoon model predicted.[9] Second, the available energy dissipation into vibration of the product, particularly for KH and RbH, generally increased with the principal quantum number. Third, more than 70% of the available energy was released as translation. Finally, the rotational populations of the alkali hydrides were in statistical thermal distributions. The behavior of alkali atom-H_2 reactions reveals marked differences from other reactions, such as those of an alkali atom with halogen-containing molecules.[24,25] Although the harpoon mechanism is applicable to both types of reactions, the latter type, containing reactants with a substantial electron-withdrawing character, may lead to a substantial partition of total available energy into vibration, but not translation, as observed in the former reaction.[24]

The Na $(4\,^2P)$ plus H_2 reaction is the only exception with a different reaction pathway from K, Rb, and Cs. For the Na $(4\,^2P)$ reaction, Kleiber and co-workers[4,5] found that a bimodal rotational distribution of NaH resulted with the minor component peaking at low J and the major component peaking at high J. The bimodal nature was thought to stem from a side-on attack along an attractive surface, which determined the microscopic branching late in the exit channel.[4,5,10] A minor secondary mechanism, following an end-on attack along a repulsive surface to contribute to the low rotational population, was also proposed in a far-wing scattering measurement.[4,5] To interpret the insertion preference, Bersohn suggested that the Na atom with a smaller size should suffer from the least repulsion in the insertion approach into the H–H bond.[9]

As for the reaction between Li and H_2, to the best of our knowledge, there is little information on its related dynamical behavior,[26,27] despite an abundance of spectroscopic data reported for LiH in various states.[28–30] Thanks to these spec-

[a]Permanent address: Department of Chemistry, Chinese Culture University, Taipei; electronic mail: ymhung@gate.sinica.edu.tw
[b]Author to whom correspondence should be addressed. Fax: 886-2-23621483; electronic mail: kclin@mail.ch.ntu.edu.tw

tral assignments for LiH, we report for the first time detailed information on the reaction pathway and rotational state distribution of the LiH product ($v=0$) as a result of the Li($2\,^2P_J$) with a H_2 reaction. Li($2\,^2P_J$) is the first excited state; its reaction with H_2 is endothermic by 1624 cm^{-1}.[27] The corresponding reaction cross section has been reported to be as small as 0.1 ± 0.03 Å^2 at 788 K.[31] However, the H_2 collision-induced quenching process has been found to occur at a gas kinetic rate. Berry and Berry have reported the quenching cross section to be 40.7 Å^2 for Li($2\,^2P_{1/2}-2\,^2S_{1/2}$) at 564 K.[32] Jenkins obtained a value of 18.4 Å^2 at 1400 K.[33] Lin and Weston obtained a value of 24.3 Å^2 by photodissociation of LiI with radiation at 220 nm.[34] The obtained electronic quenching efficiencies of Li($2\,^2P_J$) by H_2 are relatively larger than those reported for Na and K in their lower lying states.[33,35–38] Whether such abnormal quenching behavior will be reflected in the chemical reaction is an interesting issue not yet known. Therefore, in this work we seek to find the reaction mechanism for the Li($2\,^2P_J$) with a H_2 reaction.

In spite of the endothermicity of the Li($2\,^2P_J$) plus H_2 reaction, in this work a nascent rotational population distribution of LiH($v=0$) has been found to yield a single rotational temperature of ~770 K. The result is hotter by 90 K than the system temperature. The rotational distribution appears similar to those formed by the K, Rb, and Cs reactions with H_2, but differs from the Na reaction, which yields a bimodal distribution. The reaction may proceed via a nonadiabatic transition to the ground state surface. With the aid of the potential energy surface calculations, the reaction mechanism is found to favor a side-on attack of Li insertion into the H–H bond. The reaction barrier is evaluated to be 1280 cm^{-1} from the measurement of the temperature dependence. This implies that the activation barrier is approximately equivalent to the endothermicity of the system. The Li($3\,^2S$,$3\,^2P$) reactions have also been initiated, but no LiH products were detectable. In contrast to this fact, increased reactivity has been found in the other alkali elements with increased excitation energy, suggesting a marked difference in the reaction pathway for other alkalis compared to Li.

II. EXPERIMENTAL

The experimental apparatus is similar to the one used previously,[12,13,15] employing a pump–probe technique in a bulb system. The pump beam was a 10 Hz, 5–8 ns pulsed doubled Nd:YAG laser-pumped dye laser, which was used to prepare the Li atom in the $2\,^2P$, $3\,^2S$, and $3\,^2P$ states. With the use of a dye mixture of DCM and LDS698 in a volume ratio of 1:1 and a DCM dye (doubled), the $2\,^2P_J$ and $3\,^2P$ states were excited at 670.9 and 323.4 nm, respectively, while the $3\,^2S$ state was excited via a two-photon absorption at 735 nm with LDS750 dye. The probe dye laser with a B-PBD dye, pumped by another (tripled) Nd:YAG laser, was used to excite the laser-induced fluorescence (LIF) spectra of the LiH product in the $A\,^1\Sigma^+-X\,^1\Sigma^+$ transition from 360 to 380 nm. The LIF of LiH ($v=1$) was excited with a PBBO dye laser from 383 to 393 nm. The unfocused pump and probe beams propagating opposite to each other were collimated via an individual pinhole of 0.3 cm^2 cross section. The output energies for both beams were kept less than 200 μJ in order to prevent unwanted multiphoton excitation to any higher states or optical saturation of the LIF. The probe beam was spatially delayed about 10 ns. The zero delay time was defined as the maximum temporal overlap between the pump and probe pulses. Therefore, adjustment of a brief delay time would avoid the occurrence of two-color multi-photon excitation processes, and also ensured that the product population distribution would be in a nascent state. The measurement of delay time dependence indicated that the relative intensities of overall signals in the various distributions were similar to each other within 20 ns at a pressure of 10 Torr, but the corresponding signal-to-noise ratio for a briefer time delay was poor. The rotational line (6, 0) R5 was selected for the measurement of the H_2-pressure dependence. Its peak area was linearly proportional to the H_2 pressure up to 15 Torr at a 10 ns time delay, implying that the rotational cooling and secondary reaction processes were negligible.

A six-armed heat-pipe oven was used to contain the Li metal, which was heated to 680 ± 1 K. The Li vapor pressure corresponded to 8–10 mTorr. The chamber was evacuated to 10^{-5} Torr prior to the introduction of H_2. The H_2 gas, regulated at a constant pressure of about 10 Torr monitored by a MKS capacitance pressure gauge, flowed slowly through the chamber. For the temperature dependence of the rotational line intensity, the temperature was varied from 610 to 760 K, as monitored with a thermocouple intruding into the reaction region, while the H_2 gas inside the chamber was regulated at a constant pressure.

For detecting the LiH($v=0$) population at 680 K, the (5,0), (6,0), (7,0), and (8,0) [(v',v'')] bands were excited while emissions from the (5,5), (6,6), (7,7), and (8,8) bands were monitored. Such a LIF detection took advantage of the Franck–Condon factors calculated.[29] The obtained LIF signal of LiH was transmitted perpendicularly relative to the laser beam through a monochromator and detected by a photomultiplier tube enclosed in a cooler at -20 °C. The monochromator functioned as a filter to reduce interference from scattered light. An additional photomultiplier tube was attached on the opposite side of the reactor, relative to the other detector, for recording simultaneously the atomic Li emission in the $2\,^2P_J\rightarrow2\,^2S$ transition from the reaction region. The LIF signal of LiH was normalized to the intensity of the Li emission to maintain the factor of the Li density unchanged throughout the experiment. For the measurement of temperature dependence, such a normalization treatment is necessary; otherwise the reactant concentration may increase with temperature.

III. POTENTIAL ENERGY SURFACE CALCULATIONS

For a better understanding of the reaction pathway for this reaction, we have conducted calculations of *ab initio* potential energy surfaces. The calculation method adopted has been described in detail by Jeung and co-workers.[27] The basis sets used were $9s8p5d3f/4s3p$ with the first four s functions of Li and the first two s functions of H contracted from the original $12s8p5d3f/5s3p$.[27] The calculations were carried out using the MOLPRO program. This work involved 3 active electrons and 12 active spaces in complete active

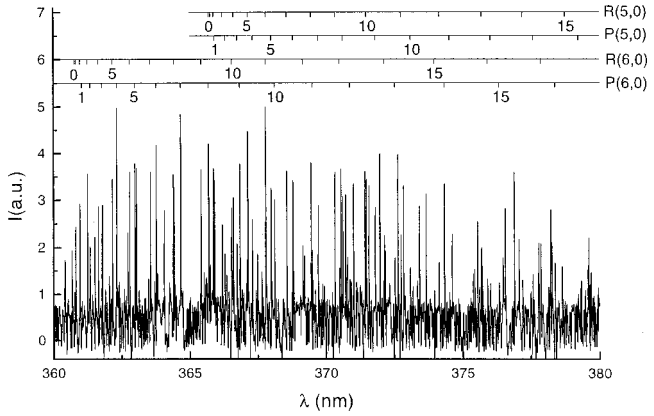

FIG. 1. LIF spectra of LiH $(v=0)$ in the $A\,^1\Sigma^+-X\,^1\Sigma^+$ transition. The vibrational levels, $v'=5$, 6, 7, and 8, in the upper state are populated and the emissions from the (5,5), (6,6), (7,7), and (8,8) bands are monitored, respectively.

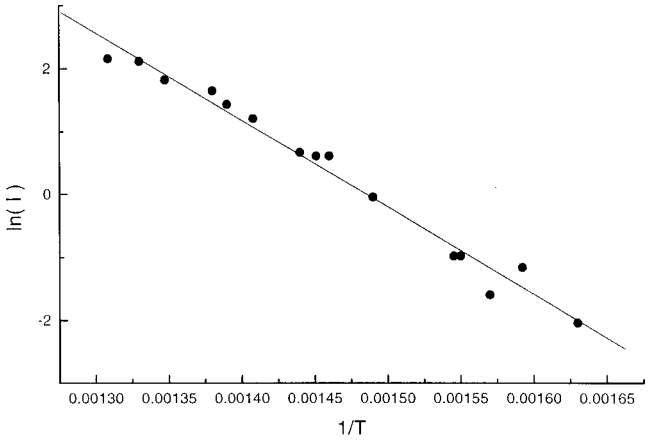

FIG. 3. The peak area of the rotational line (6, 0)R5 as a function of the reciprocal of the temperature in the range from 610 to 760 K. The slope yields information on the activation energy, according to the Arrhenius theory.

space self-consistent field (CASSCF) calculations. The molecular orbitals (MOs) were optimized for the average of all the states made from this active space. Then multireference single and double configuration interaction (MRCI) calculations were done using the MOs resulting from the CASSCF calculations, using the same active space. Two-core electrons in Li $(1s^2)$ were involved in the single excitation calculations to include the valence-core correlation effect. With this method, the calculated molecular constants for the H_2 and LiH molecules have resulted in good agreement with experimental observations.[27]

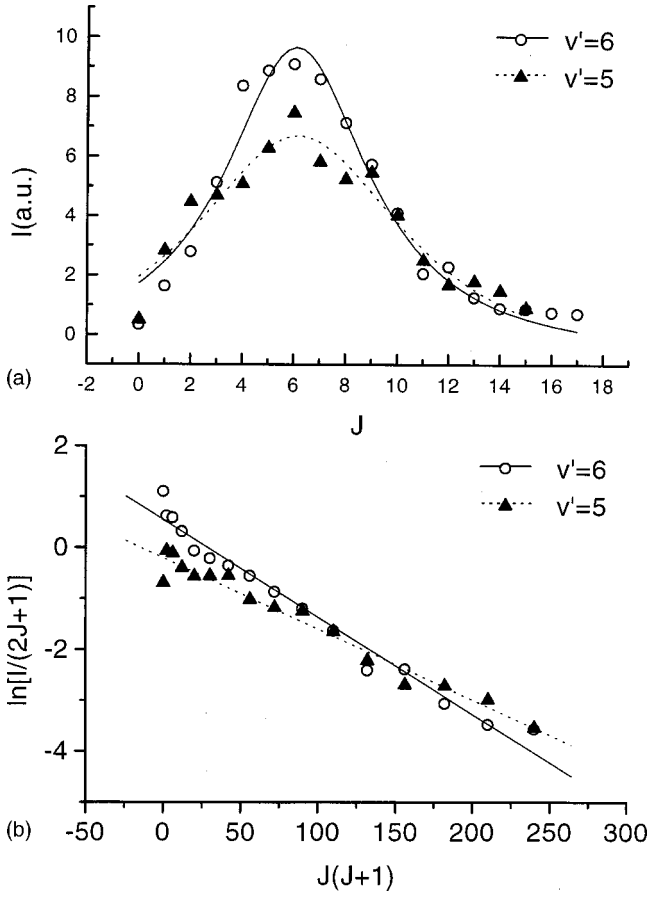

FIG. 2. (a) Rotational population distributions of LiH $(v=0)$ determined from the (5,0) and (6,0) bands. (b) Plot of $\ln[I/(2J+1)]$ as a function of $J(J+1)$; I denotes the peak area of the rotational line and J, the rotational quantum number. The slopes obtained are characterized by the Boltzmann rotational temperature.

IV. RESULTS AND DISCUSSION

A. Rotational population distribution of LiH

Excitation spectra of LiH (5,0), (6,0), (7,0), and (8,0) bands in the $A\,^1\Sigma^+-X\,^1\Sigma^+$ transition is shown in Fig. 1, as the Li $2\,^2P$ state is excited at 670.9 nm. The obtained spectra are in a nascent state, as examined by the measurements described in Sec. II. The spectral assignments of these rovibrational bands are consistent with the predicted counterpart within 1 cm^{-1}, adopting the molecular constants for the X and A states reported by Stwalley and co-workers.[28–30] Figure 1 gives partial assignment of only the (5,0) and (6,0) bands, containing the rotational lines up to $J=15$ and 17, respectively. By taking into account the Hönl–London factors, the rotational population distributions of LiH $(v=0)$, as represented by the average intensities of P and R branch lines, are displayed in Fig. 2(a). The distributions appear to be monomodal, peaking at $J=6-7$. The rotational population may be approximately characterized by a statistical thermal distribution. As shown in Fig. 2(b), a plot of the peak area of each line against $J(J+1)$ yields a slope corresponding to a rotational temperature of 778 ± 37 and 762 ± 54 K estimated from the (5,0) and (6,0) bands, respectively. The $v\geqslant1$ populations were not detectable (<0.05 Å^2), since for such an endothermic reaction, it is difficult to have enough energy to populate any higher vibrational levels. In addition, as the Li $3\,^2S$ and $3\,^2P$ states are excited, respectively, no detectable LiH product is observed (<0.05 Å^2).

Note that the spectral resolution of our laser systems cannot distinguish between two levels of the $2\,^2P_J$ doublet, separated by 0.34 cm^{-1}. In addition the cross section for fine-structure mixing by H_2 has been measured to be 54.5 Å^2 for the transition $2\,^2P_{3/2}\leftarrow2\,^2P_{1/2}$ and 26.9 Å^2 for the reverse

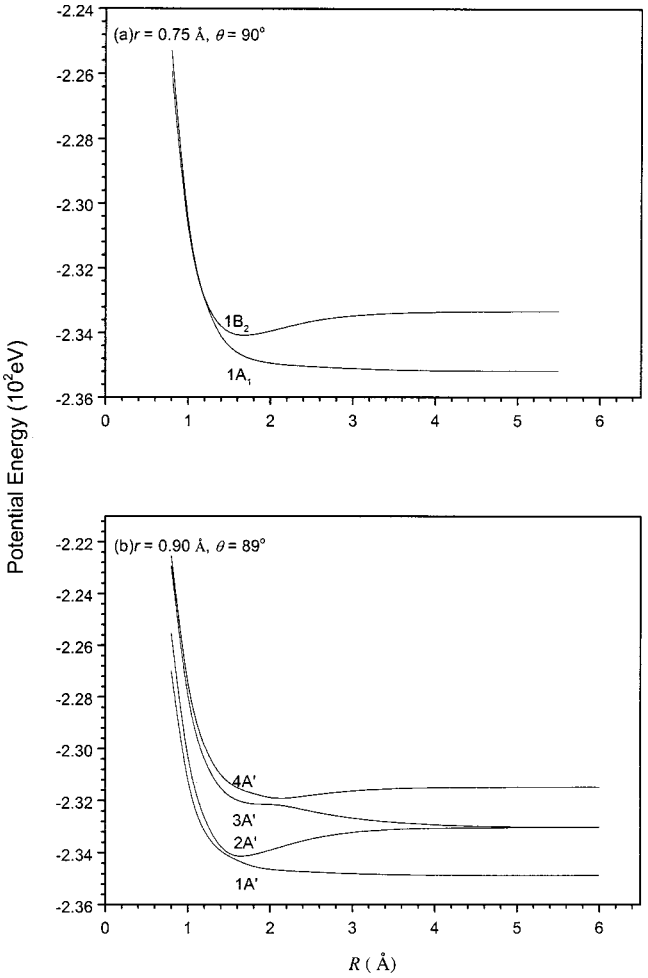

FIG. 4. (a) Energies of the $1A_1$ and $1B_2$ surfaces, correlating with the Li $2\,^2S$ and $2\,^2P$ states, as a function of the distance R between Li and the center of the H_2 bond, calculated in a C_{2v} symmetry. The H_2 bond length is fixed at 0.75 Å, the equilibrium distance. (b) Energies of the $1A'$, $2A'$, $3A'$, and $4A'$ surfaces, calculated in a near C_{2v} symmetry (angle=89°). The H_2 bond length is stretched to 0.9 Å. The $3A'$ and $4A'$ surfaces correlate with the Li $2\,^2P$ and $3\,^2S$ states, respectively.

process.[32] Such a large mixing cross section should make the spin–orbit effect negligible on the rotational distribution.

As for the temperature effect, the rotational line (6, 0)R5 is selected for the measurements. Its peak area is plotted against the reciprocal of the temperature on a semilogarithmic scale. Note that the rotational line intensity used here has been normalized to the atomic line intensity of the Li $(2\,^2P_J)$ emission, as described in Sec. II. According to Arrhenius theory, the slope shown in Fig. 3 yields an energy barrier of $1280 \pm 46\ \mathrm{cm}^{-1}$. The value is less than the endothermic energy, which is 1624 cm^{-1} calculated by Jeung and coworkers. They have considered the zero-point energies for the reactants and products, but neglected the kinetic and internal energies of the system.[27]

B. Reactive and inelastic quenching mechanisms

With the H–H bond fixed at 0.75 Å, Fig. 4(a) shows the potential curves for the $1A_1$ and $1B_2$ surfaces in C_{2v} geometry as a function of the distance, R, between Li and the center of H_2. The curve crossing occurs in the short interactive range at a distance of 1.2 Å. The energy at the crossing point appears to be about 4300 cm^{-1} larger than that for separated reactants. In contrast, the crossing region moves outward to a distance of 1.6 Å in the attractive region of the $2A'$ surface, as the H_2 bond is stretched to 0.9 Å, as shown in Fig. 4(b). When the relative energy of LiH_2 along the $1B_2$ surface is calculated at $R = 1.2$ Å, near the curve crossing, as a function of the HLiH angle, the barrier increases as the angle decreases from 90° to 10°. As shown in Fig. 5, the relative energy difference may be up to 4–5.5 eV, depending on the H_2 bond length. Therefore, the reaction pathway favors Li insertion into the H_2 bond. The colliding species follows a near C_{2v} coordinate to the attractive region and then couples to the lower state from which the products are formed. The prediction is consistent with those reported previously.[26,27] The obtained high rotational temperature can thus be reasonably interpreted as rising from a rotational torque generated as one H atom is removed from the bent collision complex. If the reaction is assumed to prefer a collinear collision, then low rotation and high vibration of LiH may be otherwise obtained.

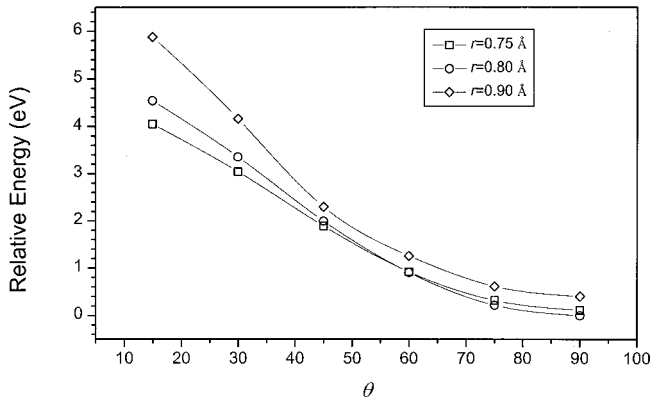

FIG. 5. A comparison of the relative energy near the crossing region between the $1A'$ and $2A'$ surfaces as a function of the HLiH angle from 90° (C_{2v} symmetry) to 10° (close to $C_{\infty v}$). The energy is calculated at a distance, $R = 1.2$ Å, between Li and the center of the H_2 bond. The H_2 bond length is fixed at 0.75, 0.8, and 0.9 Å, respectively.

There is an alternative but inefficient mechanism proposed to explain the reaction product. That is, when the Li $(2\,^2P)$ approaches H_2 along the $1B_2$ surface as the entrance channel, the Li–H_2 surface may undergo a nonadiabatic transition to the product channel LiH$(X\,^1\Sigma^+)$+H in a (near) $C_{\infty v}$ symmetry. As shown in Fig. 6(a), the LiH energy curves vary with the distance between Li and the center of H_2. Here the H–H distance is fixed at 6 Å, where the H–H bond is considered to have broken apart completely. The curve crossing may occur around 4.6 Å. For the $1A'$ surface at this point, the ground state LiH is at 1.6 Å, the equilibrium distance. The Li $(2\,^2P)$–H_2 distance at the curve crossing is still far enough to allow for an angle change from the C_{2v} to $C_{\infty v}$ collision geometry with an energy barrier less than 0.03 eV. Therefore, according to the Landau–Zener theory, it is probable for the nonadiabatic transition from the $1B_2$ surface to the $1A'$ surface to occur. However, as the kinetic energy of the colliding species increases, the transition probability should decrease, thus leading to a smaller reaction cross sec-

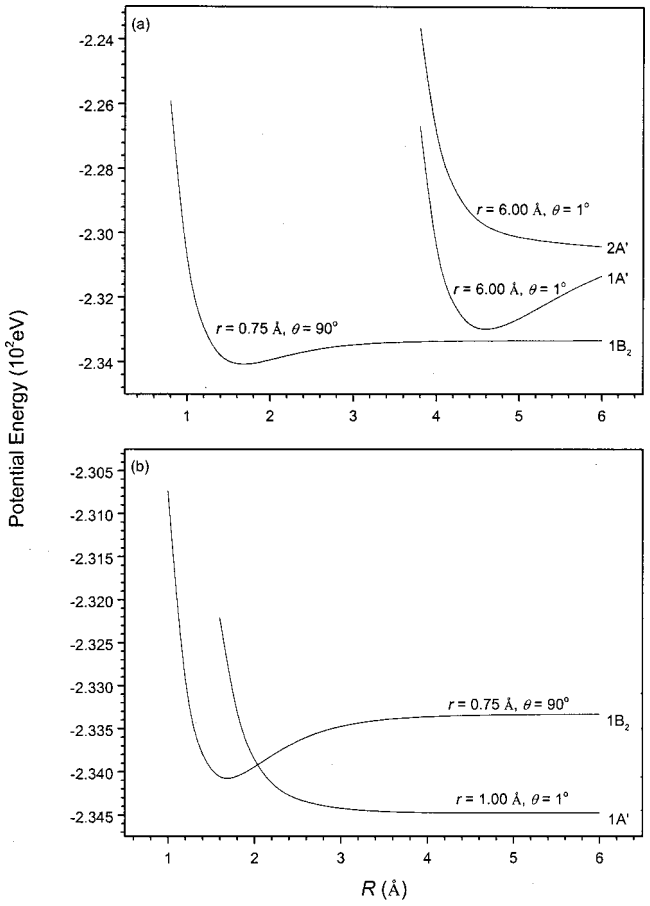

FIG. 6. (a) Energies of the $1B_2$, $1A'$ (HLiH angle$=1°$, close to $C_{\infty v}$), and $2A'$ surfaces for the Li–H_2 collision as a function of the distance R between Li and the center of the H_2 bond. The H_2 bond length is fixed at 0.75 Å for the $1\,^2B_2$ surface, while the H_2 bond length is fixed at 6 Å for the $1A'$ and $2A'$ surfaces. (b) Energies of the $1B_2$ and $1A'$ (HLiH angle$=1°$, close to $C_{\infty v}$) surfaces for the Li–H_2 collision as a function of the distance R between Li and the center of the H_2 bond. The H_2 bond length is fixed at 0.75 Å for the $1\,^2B_2$ surface, while the H_2 bond length is fixed at 1 Å for the $1A'$ surface.

tion. This prediction is contrary to our experimental results of the temperature effect. Such a long-range nonadiabatic curve crossing should be negligible.

As reported previously, the $1A'$ and $2A'$ surfaces cross along a line seam where the colliding configuration is in C_{2v} symmetry.[27] The crossing seam around 1.6 Å is in the attractive region of the $2A'$ surface (also shown in Fig. 4).[27] With the aid of the PES calculations, the observation of the inelastic quenching cross sections, as reported to decrease with increasing temperature, may be interpreted readily. Martinez has used a multiple spawning technique to describe semiclassical nuclear dynamics and found that the nonadiabatic transitions along the line seam are extraordinarily fast, but the quenching efficiency is greatly diminished by recrossing from the lower to the upper adiabatic surface.[26] There may exist additional quenching channels to interpret the abnormally large cross sections,[32–34] as compared to those for other low-lying alkali atoms. In the following we propose an alternative quenching mechanism. As shown in Fig. 6(b), Li $(2\,^2P_J)$ and H_2 collide along a C_{2v} coordinate as the entrance channel, while the exit channel leads to the products Li $(2\,^2S)$ and H_2 along a (near) $C_{\infty v}$ coordinate. A curve crossing occurs in the attractive region of the $1B_2$ surface and the position of curve crossing depends on the H_2 bond length in the exit channel. For instance, in Fig. 6(b) the crossing point is at ~2 Å when the H_2 bond is stretched to 1.0 Å. The crossing point will move outward with an increase of the H_2 bond length. This implies that the inelastic quenching processes may take place at a large impact parameter. In addition, as the kinetic energy of the colliding species increases with temperature, the nonadiabatic transition becomes smaller, thereby leading to a smaller quenching cross section. The additional mechanism proposed might explain a much larger quenching cross section observed as well as the related temperature effect.

C. Comparison of reaction mechanisms among alkali elements

The mechanisms with a H_2 reaction among Na, K, Rb, and Cs differ from each other. Kleiber and co-workers[4,5] have demonstrated that the Na $(4\,^2P)$ reaction preferentially follows a side-on attack toward the hydrogen molecule, leading to a bimodal rotational distribution of the NaH product. The Na $(4\,^2P)-H_2$ reaction may proceed along an attractive $3\,^2B_2$ surface, which evolves through a series of surface crossings and finally joins the reactive $1\,^2B_2$ surface.[4,5,10] In contrast, K, Rb, and Cs are dominated by an electron transfer along a colinear approach geometry. Among these alkali elements, their atomic size may be an important factor to determine the preference of reaction pathways.[9] Na with a relatively small size tends to insert into the H_2 bond. However, for the K, Rb, and Cs elements with a larger size, the insertion approach may encounter large repulsion.

The other important factor to affect the mechanism is the excitation energy. From the energetic point of view, an atomic reactant in a highly excited state, which helps lower the ionization potential, may enhance the rate of the electron transfer process. For instance, Ca$(^1S_0)$ in a reaction with H_2O_2 proceeds via a long-lived neutral complex, whereas the Ca(^3P_j) reaction is dominated by a process of electron transfer.[39] The Mg $(3\,^1P_1)-H_2$ reaction favors an insertion mechanism,[40–43] whereas the Mg $(4\,^1S_0,3\,^1D_2)-H_2$ reactions are believed to proceed via a harpoon-type process.[44,45] Such a competition between insertion and harpoon mechanisms has also been found in other alkaline earth atoms with OH-containing molecules.[46] Comparing the ionization potentials among the excited states of Na, Rb, K, and Cs studied so far, the Na $(4\,^2P)$ atom is the most difficult to be ionized. The competition of pathways accordingly favors the insertion mechanism.

By analogy with the case of Na$(4\,^2S,4\,^2P)$, the Li $(2\,^2P_J)$ plus H_2 reaction is dominated by an insertion mechanism. Again, the small atomic size of Li causes the least repulsion in the insertion approach. An efficient electron back-donation from the metal atom to the antibonding σ^* of the hydrogen molecule, which may energetically stabilize the $^2B_2$ (or $^2A'$) potential surface, is another important factor to favor the insertion mechanism. Similar energetic

stabilization has also been found in the Mg$(3\,^2P)$ plus H_2 reaction.[40–42] Despite the similarity between the reactions of Li and Na, their resultant rotational state distributions are different. It is more complicated to understand the rotational bimodality for the Na case, since the product channel involves a series of curve crossings. For Li, the reaction should occur via the $2A'-1A'$ nonadiabatic transition. Therefore, the rotational distribution in the exit channel may depend on the anisotropy of the $1A'$ surface.

From the reported PES information, two aspects may be discerned. First, concerning the lack of LiH$(v>0)$ population, one may consider this from a viewpoint other than the endothermicity. As reported, the collision configuration at the crossing seam is a bent geometry with the LiH bond ($\sim$1.57 Å) close to the equilibrium distance.[27] If one hydrogen atom departs impulsively from the LiH_2 complex, the impulse force should cause the available energy conversion into vibration to be relatively small. Second, the anisotropic feature of the ground state surface may affect the obtained rotational temperature. As compared to the case of the Mg$(3\,^2P)$ plus H_2 reaction, the rotational temperature obtained in this work is much smaller than that corresponding to the high rotational component of the MgH distribution. For the case of Mg, the colliding species following the surface transition may decompose via a collinear HMgH intermediate complex.[40–43] The strong anisotropic interaction results in the higher rotational component of the bimodal distribution. In contrast, for the case of Li, although the detailed $1A'$ PES is unknown, we expect that the minimum energy of the LiH_2 complex on the surface should be in a bent configuration, similar to that calculated for the $4A'$ surface correlating with the Li $3\,^2S$ state.[27] Thus, upon the transition to the lower surface, the LiH_2 collision complex, which decomposes via a bent intermediate, is subject to a relatively weak anisotropic interaction.

As reported previously, the higher-lying states of alkali atoms are very reactive toward the hydrogen molecule. The relative reactivity for the high-lying K atoms follows an order of $D<P<S$.[12,13] Similarly, in the Rb$(5\,^2D,7\,^2S)$ with H_2 reactions, Luh and co-workers have found that the chemical reactivity follows the order of $5\,^2D_{1/2}<5\,^2D_{3/2}<7\,^2S_{1/2}$.[16] However, Vetter and co-workers have found that the reactivity between the ^2S and ^2D state is reversed in the Cs case.[23] A combination of atomic orbital symmetry, steric barrier, and energetic effects have recently been proposed to account for the state reactivities observed.[14,15]

To our surprise, unlike the reactivity for the above high-lying alkali atoms, the chemical reaction initiated by the Li atoms in the $3\,^2S$ or $3\,^2P$ states cannot be detected. From the PES calculations reported[27] and also conducted in this work, when the Li$(3\,^2S)$ atom approaches H_2 in near C_{2v} symmetry, the $4\,^2A'$ surface can feasibly couple to a repulsive $3A'$ surface. The repulsion is exerted on the collision complex to make the moiety break up into the products [Li$(2\,^2P_J)$ $+H_2$] along the $3A'$ surface. The probability for further surface hopping from the $3A'$ to the $2A'$ surface should be negligible, since their PES are separated too far from each other to have a significant coupling (also see Fig. 4). The Li$(3\,^2P)$ state is expected to behave similarly. The forbidden reaction found in the high-lying Li states implies that the harpoon mechanism cannot be dominant in this system.

IV. CONCLUSION

In this work we have provided insight into the dynamical behavior for the Li$(2\,^2P_J)$ with a H_2 reaction. The obtained nascent rotational population distribution of LiH$(v=0)$ yields a single rotational temperature about 90 K higher than the system temperature. LiH in the $v=1$ level is not detectable. By combining the PES calculations and the observations, we believe that the current reaction should be dominated by the insertion mechanism. This reaction pathway is similar to the case of Na$(4\,^2P)$, but the latter leads to a bimodal rotational distribution. The activation energy has been determined by temperature dependence measurements. Regardless of the initial energy carried by the reactants, the obtained barrier suggests that the endothermic energy is the only barrier for the reaction.

The reaction behavior for the high-lying Li atoms differs from those for the high-lying K, Rb, and Cs atoms. The Li$(3\,^2S,3\,^2P)$ reactions with the hydrogen molecule do not lead to any detectable LiH product. It may be reasonably interpreted that the corresponding $4A'$ and higher surfaces may not effectively couple to the reactive $2A'$ and $1A'$ surfaces. The observation provides indirect evidence that the harpoon mechanism cannot be applied to the Li reaction. It is otherwise probable for the Li$(3\,^2S,3\,^2P)-H_2$ collision to enter the ion-pair surface that may join the $2A'$ and $1A'$ surfaces. This conclusion is also supported by Jeung and coworkers from a theoretical point of view.[27]

ACKNOWLEDGMENTS

Y.M.H. and K.C.L. wish to thank Professor G. H. Jeung for his hospitality during Y.M.H.'s stay in his lab, and for generously providing the basis sets and programs used in the PES calculations. This work was supported by the National Science Council and the Chinese Petroleum Company, the Republic of China, under Contract No. NSC-89-2113-M-001-084.

[1] C. Crepin, J. L. Picque, G. Rahmat, J. Verges, R. Vetter, F. X. Gadea, M. Pelissier, F. Spiegelmann, and J. P. Malrieu, Chem. Phys. Lett. **110**, 395 (1984).
[2] J. P. Visticot, M. Farray, J. Lozingot, and B. Sayer, J. Chem. Phys. **79**, 2839 (1983).
[3] A. G. Urena and R. Vetter, Int. Rev. Phys. Chem. **15**, 375 (1996).
[4] S. Bililign, P. B. Kleiber, W. R. Kearney, and K. M. Sando, J. Chem. Phys. **96**, 218 (1992).
[5] S. Bililign and P. D. Kleiber, J. Chem. Phys. **96**, 213 (1992).
[6] J. Cuvellier, L. Petitjean, J. M. Mestdagh, D. Paillard, P. de Pujo, and J. Berlande, J. Chem. Phys. **84**, 1451 (1986).
[7] K. C. Lin and H. C. Chang, J. Chem. Phys. **90**, 6151 (1989).
[8] H. C. Chang, Y. L. Luo, and K. C. Lin, J. Chem. Phys. **94**, 3529 (1991).
[9] X. Huang, J. Zhao, G. Xing, X. Wang, and R. Bersohn, J. Chem. Phys. **104**, 1338 (1996).
[10] A. Sevin and P. Chaquin, Chem. Phys. **93**, 49 (1985).
[11] Y. L. Luo, K. C. Lin, D. K. Liu, H. J. Liu, and W. T. Luh, Phys. Rev. A **46**, 3834 (1992).
[12] D. K. Liu and K. C. Lin, J. Chem. Phys. **105**, 9121 (1996).
[13] D. K. Liu and K. C. Lin, J. Chem. Phys. **107**, 4244 (1997).
[14] T. H. Wong and P. D. Kleiber, J. Chem. Phys. **110**, 6743 (1999).
[15] Y. C. Hsiao, D. K. Liu, H. S. Fung, and K. C. Lin, J. Chem. Phys. **113**, 4613 (2000).

[16] L. H. Fan, J. J. Chen, Y. Y. Lin, and W. T. Luh, J. Phys. Chem. A **103**, 1300 (1999).
[17] M. L. Chen, W. C. Lin, and W. T. Luh, J. Chem. Phys. **106**, 5972 (1997).
[18] J.-M. L'Hermite, G. Rahmat, and R. Vetter, J. Chem. Phys. **93**, 434 (1990).
[19] F. X. Gadea, J. M. L'Hermite, G. Rahmat, and R. Vetter, Chem. Phys. Lett. **151**, 183 (1988).
[20] F. X. Gadea, F. Spiegelmann, M. Pelissier, and J. P. Malrieu, J. Chem. Phys. **84**, 4872 (1986).
[21] J. M. L'Hermite, J. Chem. Phys. **97**, 6215 (1992).
[22] A. G. Urena and R. Vetter, J. Chem. Soc., Faraday Trans. **91**, 389 (1995).
[23] V. Cavero, J. M. Lmermite, G. Rahmat, and R. Vetter, J. Chem. Phys. **110**, 3428 (1999).
[24] D. R. Herschbach, Adv. Chem. Phys. **10**, 319 (1966).
[25] J. M. Mestdagh, B. A. Balko, M. H. Covinsky, P. S. Weiss, M. F. Vernon, H. Schmidt, and Y. T. Lee, Faraday Discuss. Chem. Soc. **84**, 145 (1987).
[26] T. J. Martinez, Chem. Phys. Lett. **272**, 139 (1997).
[27] H. S. Lee, Y. S. Lee, and G. H. Jeung, J. Phys. Chem. A **103**, 11 080 (1999).
[28] W. C. Stwalley and W. T. Zemke, J. Phys. Chem. Ref. Data **22**, 87 (1993).
[29] W. T. Zemke and W. C. Stwalley, J. Chem. Phys. **68**, 4619 (1978).
[30] F. B. Orth and W. C. Stwalley, J. Mol. Spectrosc. **76**, 17 (1979).
[31] E. G. Mysers, D. E. Murnick, and W. R. Softky, Appl. Phys. B: Photophys. Laser Chem. **43**, 247 (1987).
[32] J. E. Berry and M. J. Berry, J. Chem. Phys. **72**, 4510 (1980).
[33] D. R. Jenkins, Proc. R. Soc. London, Ser. A **306**, 413 (1968).
[34] S. M. Lin and R. E. Weston, Jr., J. Chem. Phys. **65**, 1443 (1976).
[35] B. L. Earl and R. R. Herm, J. Chem. Phys. **60**, 4568 (1974).
[36] P. L. Lijnse and J. C. Hornman, J. Quant. Spectrosc. Radiat. Transf. **14**, 1079 (1974).
[37] C. B. Ke and K. C. Lin, J. Chem. Phys. **99**, 9603 (1993).
[38] T. F. Gallagher and W. E. Cooke, Phys. Rev. A **19**, 2161 (1979).
[39] M. D. Oberlander, R. P. Kampf, and J. M. Parson, Chem. Phys. Lett. **176**, 385 (1991).
[40] W. H. Breckenridge and H. Umemoto, J. Chem. Phys. **80**, 4168 (1984).
[41] P. D. Kleiber, A. M. Lyyra, K. M. Sando, S. P. Heneghan, and W. C. Stwalley, Phys. Rev. Lett. **54**, 2003 (1985).
[42] Y. R. Ou, D. K. Liu, and K. C. Lin, J. Chem. Phys. **108**, 1475 (1998).
[43] Y. R. Ou, Y. M. Hung, and K. C. Lin, J. Phys. Chem. A **103**, 7938 (1999).
[44] D. K. Liu and K. C. Lin, Chem. Phys. Lett. **304**, 336 (1999).
[45] D. K. Liu, K. C. Lin, and J. J. Chen, J. Chem. Phys. **113**, 5302 (2000).
[46] P. de Pujo, O. Sublementier, J. P. Visticot, J. Berlande, J. Cuvellier, C. Alcaraz, T. Gustavsson, J. M. Mestdagh, and P. Meynadier, J. Chem. Phys. **99**, 2533 (1993).